Electronic Supplementary Material (ESI) for ChemComm.
This journal is © The Royal Society of Chemistry 2024

Supporting information

Selective grain boundaries passivation by ammonium nitrate for enhanced performance and stability of FA-Cs based perovskite solar cells

Xiaoshan Li,[a†] Wenjing Yu,[a,b†] Tian Hou,[a] Xin Yang,[a] Xin Wang,[a] Guangmian Jiang,[a] Zhipeng Fu,[a] Kaipeng Chen,[a] Yanlin Li,[a] Chengbin Yang,[a] Xiaoran Sun*[a], Meng Zhang*[a,c]

Author address

[a] School of New Energy and Materials, Southwest Petroleum University (SWPU), Chengdu, 610500, China

[b] Sichuan Shale Gas Project Management Department, CNPC Bohai Drilling Engineering Co. Ltd., Chengdu 610057, China

[c] The Australian Centre for Advanced Photovoltaics, School of Photovoltaic and Renewable Energy Engineering, University of New South Wales, Sydney, NSW 2052, Australia

[†] These authors contribute equally to this work

Corresponding Author

E-mail: meng.zhang@unsw.edu.au; xiaoran.sun@swpu.edu.au;

Experimental

Materials

Ammonium nitrate (NH_4NO_3, 99.85%) was purchased from aladdin. Formamidinium iodide (FAI, 99.5%), lead iodide (PbI_2, 99.99%), cesium iodide (CsI, 99.99%), spiro-OMeTAD (99.5%), bis (trifluoromethane) sulfonimide lithium salt (Li-TFSI, >99%) and 4-*tert*-butylpyridine (TBP, >96%) were purchased from Xi'an Polymer Light Technology Corp. SnO_2 colloidal solution [15%tin (IV) in H_2O colloidal dispersion] was purchased from Alfa Aesar. The solvents tetramethylene sulfoxide (TMSO, >95.0%), N, N-dimethylformamide (DMF, anhydrous, 99.8%), isopropanol (IPA, anhydrous, 99.9%), acetonitrile (anhydrous, 99.8%) and chlorobenzene (CB, anhydrous, 99.8%) were purchased from Sigma-Aldrich. All chemicals and reagents were directly used as received.

Device fabrication

ITO glass substrates were cleaned subsequently with detergent (5 vol% in deionized water), acetone, isopropanol and ethanol for 20 min respectively. The substrates were dried by N_2 gas. Prior to electron transporting layer (ETL) deposition, the substrates were further cleaned with UV-ozone for 15 min. The SnO_2 colloidal dispersion (15% in water, Alfa Aesar) diluted with deionized water (1:3 wt) with an additive of 4 vol% polyethylene glycol (Alfa Aesar) and 8 vol% Triton X-100 (Aladdin) was spin-coated on the ITO substrate at 3000 rpm for 30 s, followed by annealing at 150°C for 30 min and UV-ozone treatment for 15 min.

The $FA_{0.9}Cs_{0.1}PbI_3$-based perovskite precursor solution was prepared by mixing PbI_2 (1.5 M), FAI (1.35 M), and CsI (0.15 M) in a mixed solvent (DMF: TMSO=9:1, v/v). The perovskite precursor solution was spin-coated onto SnO_2 with a two-step spinning procedure (1,000 rpm for 5 s and 4,000 rpm for 30 s). During the second step, Gas-quenching (N_2) was sprayed on the wet film 20 s before stopping, the gas-pressure at the regulator was set to 0.3 MPa. Subsequently the deposited perovskite layer was annealed at 150 °C for 20 min. The passivation layer was prepared by dissolving 1 mg NH_4NO_3 in 1 mL IPA, and was spin-coated on top of the perovskite layer at 4,000 rpm

for 30 s. The hole transporting layer was spin-coated on top of the passivation layer at 4,000 rpm for 30 s using a spiro-OMeTAD solution dissolving 72.3 mg spiro-OMeTAD, 17.5 μL Li-TFSI stock solution (520 mg·mL^{-1} acetonitrile), 28.8 μL TBP in 1 mL chlorobenzene. After deposition, the sample was oxidized for 4 h in a pure oxygen atmosphere for 40 °C. Finally, about 100 nm sliver electrodes were prepared by thermal evaporation.

Characterization

The top-viewed scanning electron microscope (SEM) images films were observed using scanning electron microscope (FEI INSPECT F50, U.S.A.). Atomic force microscope (AFM) images were scanned by AFM (KEYSIGHT Technologies 7500). The XRD spectra of the MA-free perovskite films were measured by an X-ray diffractometer (X'Pert Pro MPD, PANalytical). Steady-state photoluminescence (PL) was characterized by a FLS980 (Edinburgh Instruments Ltd) with an excitation at 468 nm. The current-voltage (J-V) characteristics were measured by a Keithley B2901A source and the solar simulator with standard AM 1.5G (100 mW·cm^{-2}, SS-F5-3A, Enlitech) under ambient conditions. The J-V curves were measured by forward (-0.2 to 1.2 V) or reverse (1.2 to -0.2 V) scans with a delay time of 0.02 s for each point.

The *CPD* value is the contact potential difference between the metallic KPFM tip and the sample, which can be derived as work function difference between the tip and the sample by the following equation (1):[1, 2]

$$CPD = \frac{\phi_{tip} - \phi_{sample}}{e} \quad (1)$$

where ϕ_{tip} is the work function of the KPFM tip, ϕ_{sample} is the work function of the sample surface and e is the electronic charge. Calibration gives a CPD_{tip} of 0.430 V and a ϕ_{tip} of 5.03 eV for the KPFM tip.

The trap density in the perovskite films is assessed by SCLC of electron-only devices (ITO/SnO_2/Perovskite/NH_4NO_3/PCBM/BCP/Ag). The trap-filled limit voltage (V_{TFL}), from which the trap density (n_t) can be calculated by equation (2):[3]

$$V_{TFL} = \frac{qn_t L^2}{2\varepsilon\varepsilon_0} \quad (2)$$

Where ε is the relative dielectric constant of perovskite, ε_0 is the vacuum permittivity, q is the elementary charge, and L is the thickness of the perovskite film.

The average TRPL decay lifetime (τ_{ave}) can be obtained using the following equation (3):[4]

$$\tau_{ave} = \frac{A_1\tau_1^2 + A_2\tau_2^2}{A_1\tau_1 + A_2\tau_2} \quad (3)$$

Where A_1 and A_2 are constants representing the contributions of the fast and slow components, respectively. τ_1 is the fast decay process related to bimolecular recombination, and τ_2 is the slow decay process associated with trap-assisted recombination.

The humidity stability test of the devices is carried out in ambient air without humidity control, where the average RH is recorded every 12 hours.

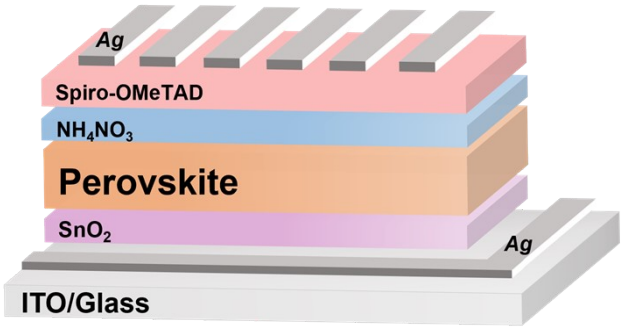

Fig. S1 Device structure of PSCs with NH_4NO_3.

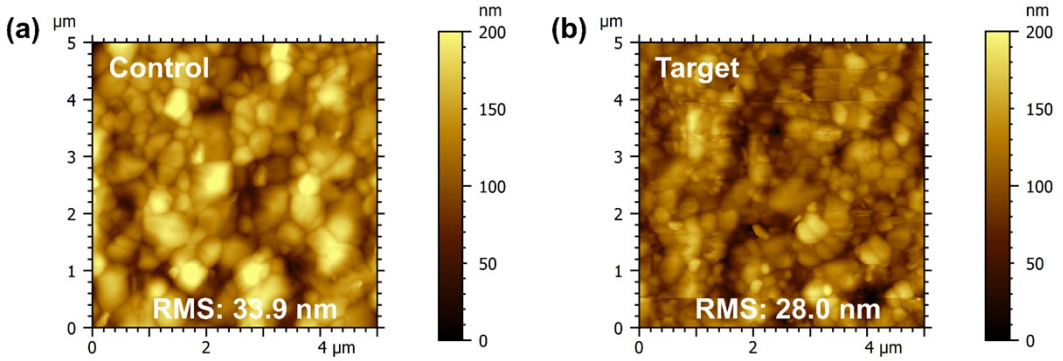

Fig. S2 (a) and (b) RMS of the perovskite film before and after NH_4NO_3 passivation by AFM.

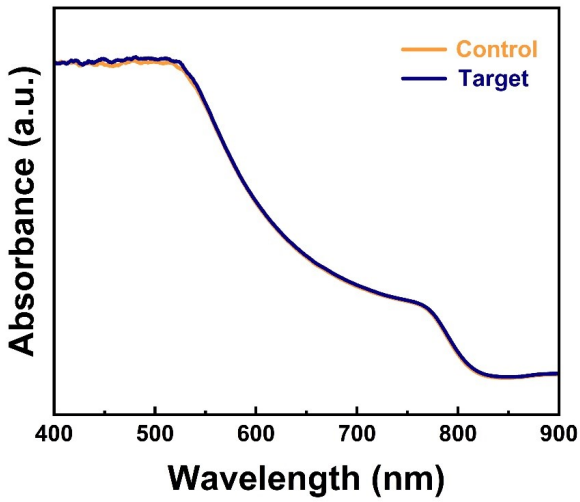

Fig. S3 UV-vis absorption spectra of pristine perovskite film, and perovskite films with NH_4NO_3 (1 mg/mL).

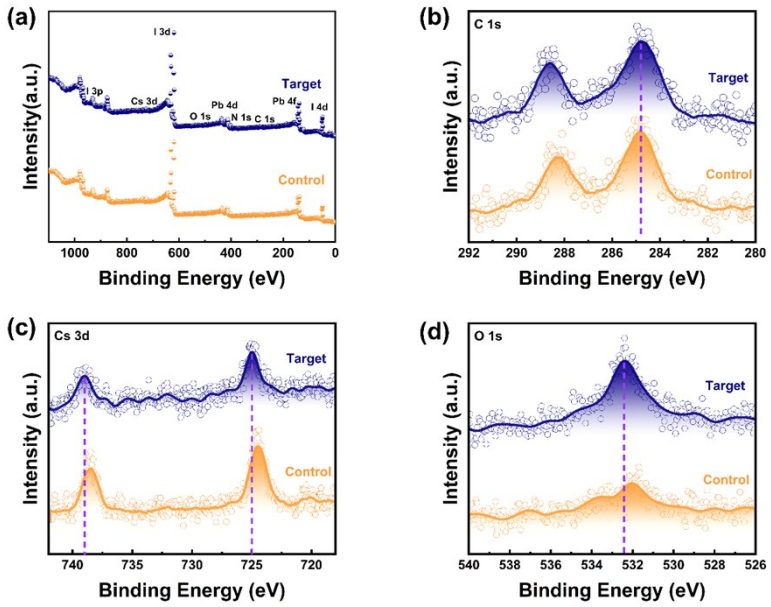

Fig. S4 XPS of control and NH_4NO_3-passivated perovskite films: (a) XPS survey spectra;(b) C 1s; (b) Cs 3d; (c) O 1s.

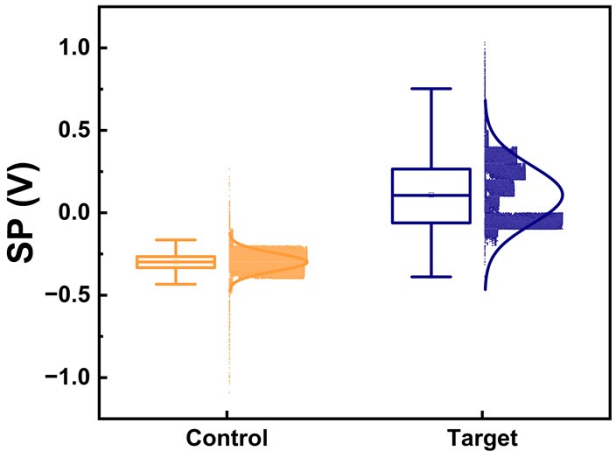

Fig. S5 The values of SP statistics for KPFM of control and NH_4NO_3-passivated films.

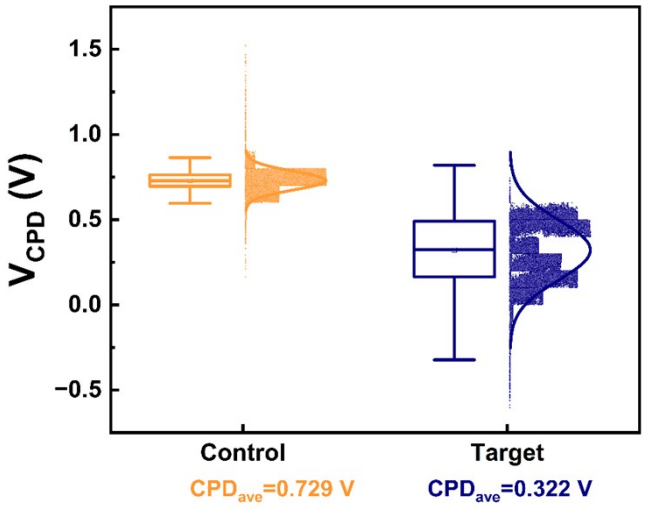

Fig. S6 The values of CPD statistics and calculations for KPFM of control and NH_4NO_3-passivated films.

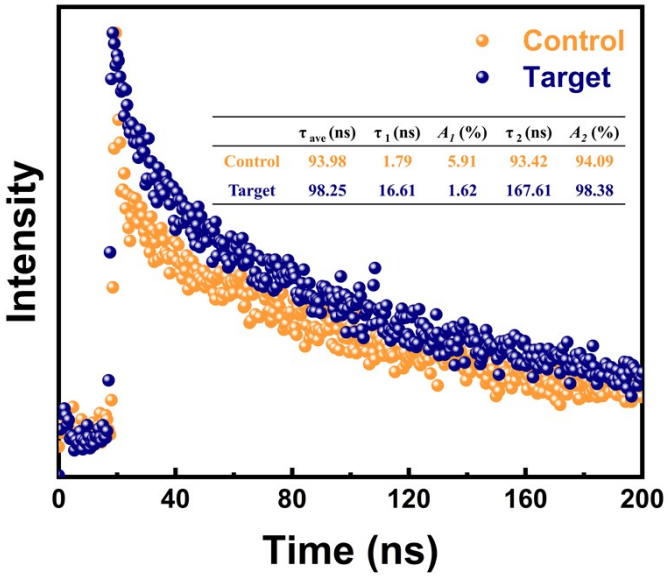

Fig. S7 TRPL to investigate the effects of NH_4NO_3 in the perovskite films.

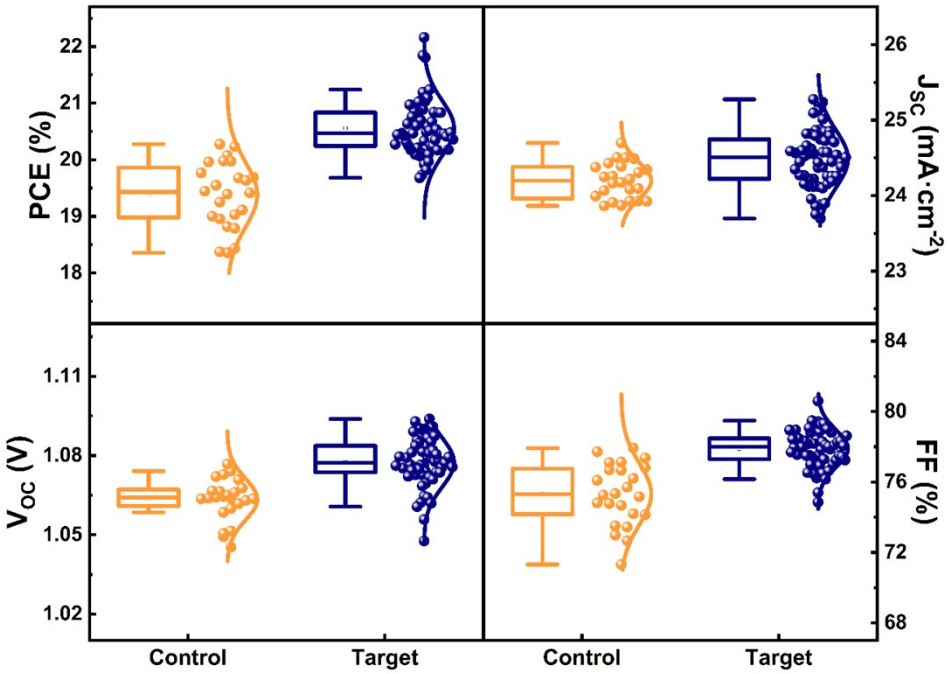

Fig. S8 J-V characteristics of with/without NH_4NO_3-passivated devices under AM1.5G simulated solar illumination.

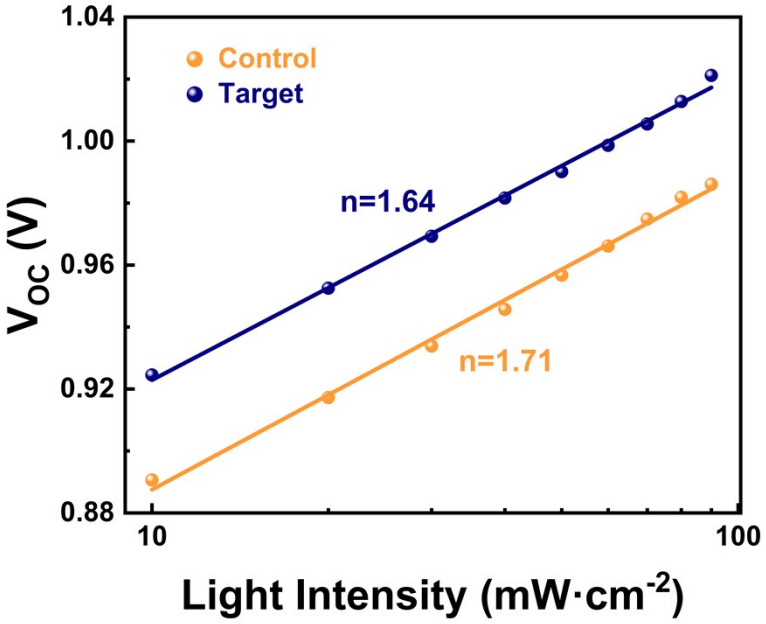

Fig. S9 Light intensity-dependent V_{OC} of the control and target devices.

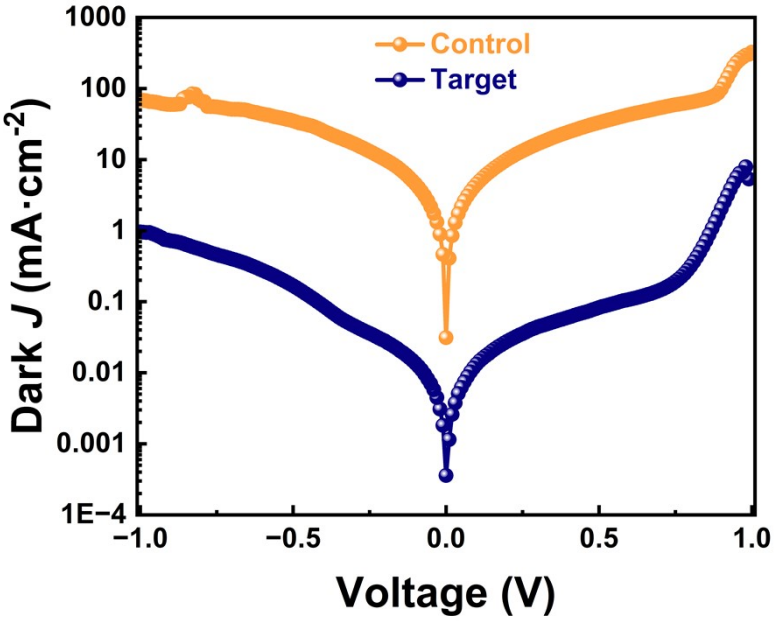

Fig. S10 Dark currents of the control and target devices.

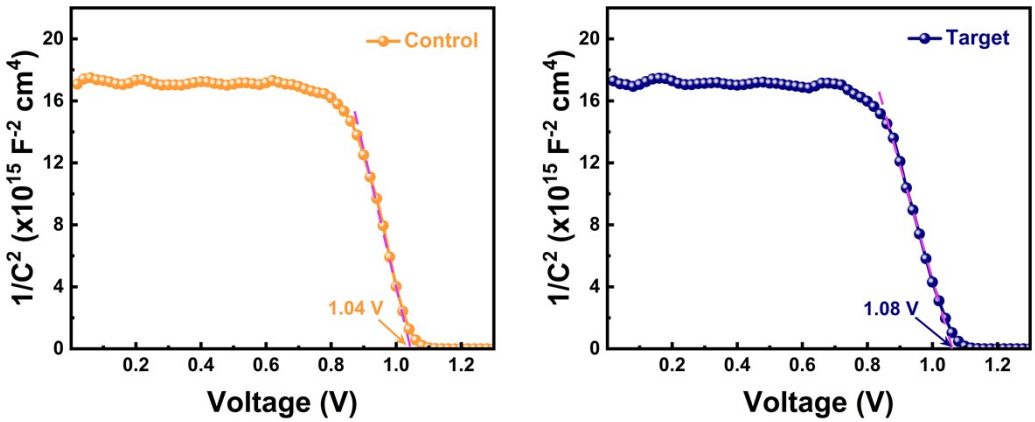

Fig. S11 Mott-Schottky curves of the control and target devices.

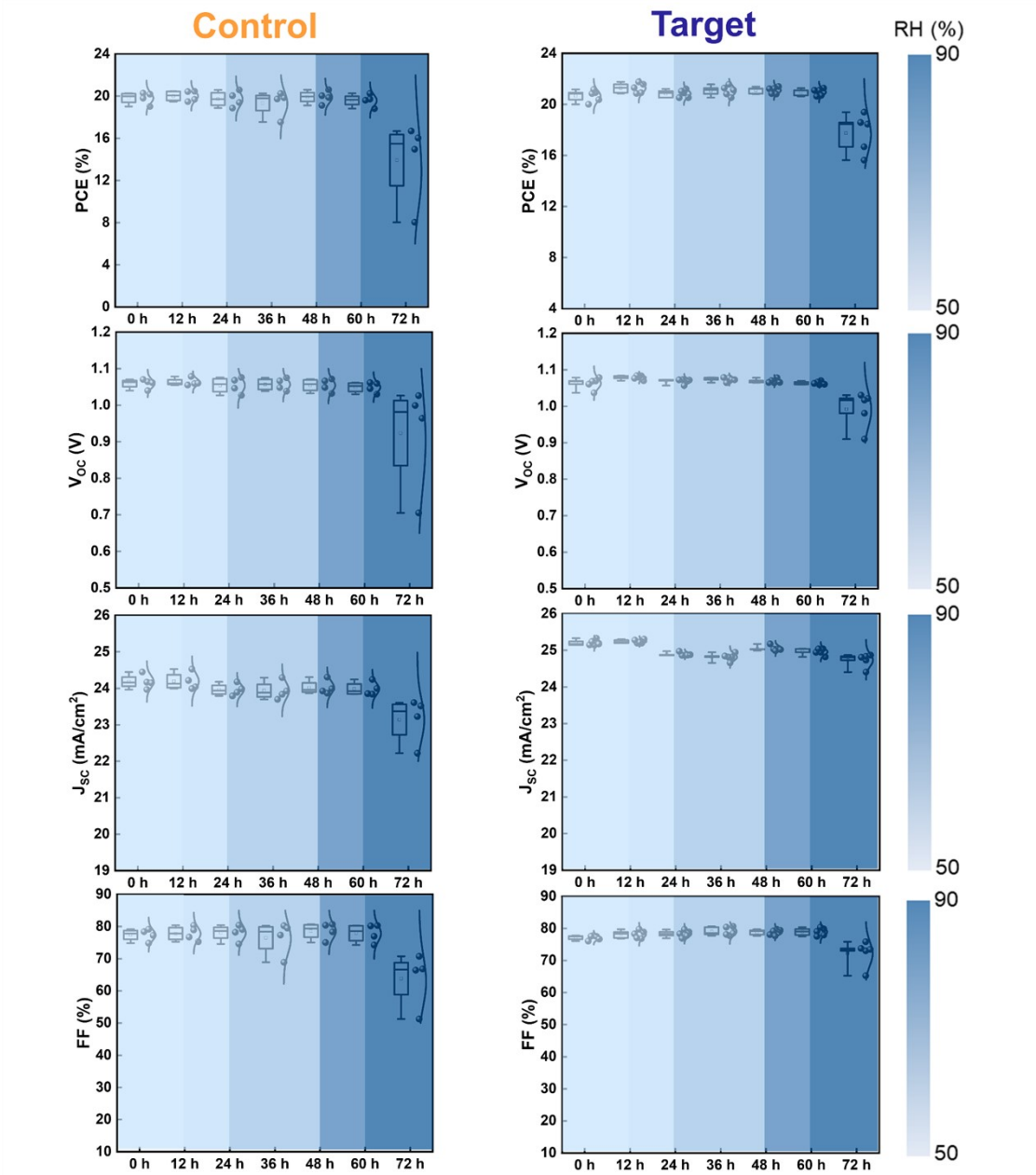

Fig. S12 Stability test based on unencapsulated devices with and without NH_4NO_3 stored in ambient air (RH=50-90%).

Table S1. Grain boundaries passivation strategies towards perovskite solar cells.

Passivator	Perovskite	Passivation methods	PCE [%] (C/P)	Ref.
poly(methyl methacrylate) (PMMA)	$Cs_{0.05}(FA_{0.9}MA_{0.1})_{0.95}Pb(I_{0.9}Br_{0.1})_3$	Surface passivation treatment	19.4/20.4	5
4-fluoro-phenethylammonium iodide (FPEAI)	$FA_{0.85}MA_{0.15}Pb(I_{0.85}Br_{0.15})_3$	Surface passivation treatment	18.46/20.53	6
3,4,5,6-tetrafluorophthalicacid (TFPA)	$FA_{0.85}MA_{0.15}PbI_3$	Surface passivation treatment	21.46/23.70	7
N-(3-aminopropyl)-imidazole diiodide (APDI)	$FA_{0.83}Cs_{0.17}Pb(I_{0.86}Br_{0.14})_3$	Surface passivation treatment	20.01/21.41	8
phenethylammonium chloride (PEACl)	$FA_{0.82}Cs_{0.18}PbI_3$	Additive and surface treatment	20.1/22.3	9
poly(bithiophene imide) (PBTI)	CsFAMA	Additive treatment	18.89/20.67	10
p-phenyl dimethylammonium iodide (PhDMADI)	$FA_{0.7}MA_{0.3}Pb_{0.5}Sn_{0.5}I_3$	Additive treatment	15.8/20.5	11
K_2SO_4	CsFAMA	Additive treatment	20.39/22.4	12
poly(6FDA-co-AHHFP (PAA)	$MAPbI_3$	Additive treatment	17.53/20.03	13
IDIS-Th	$MAPbI_3$	Antisolvent treatment	17.78/20.01	14
2-(5,6-Difluoro-3-oxo2,3-dihydro-1H-inden-1 ylidene) malononitrile (BTP-4F)	CsFAMA	Antisolvent treatment	19.25/22.16	15

Table S2. The change in PCE of devices in high humidity environments (statistics derived from 48 individual devices).

	***Start PCE$_{ave}$* (%)**	***End PCE$_{ave}$* (%)**	***Rate of decline***
Control (without NH_4NO_3)	**18.14**	**11.91**	**34.36%**
Target (with NH_4NO_3)	**19.35**	**16.26**	**15.97%**

Notes and references

1. Z. Kang, H. Si, M. Shi, C. Xu, W. Fan, S. Ma, A. Kausar, Q. Liao, Z. Zhang and Y. Zhang, *Sci. China-Mater.*, 2019, **62**, 776-789.
2. E. M. Lanzoni, T. Gallet, C. Spindler, O. Ramírez, C. K. Boumenou, S. Siebentritt and A. Redinger, *Nano Energy*, 2021, **88**, 106270.
3. A. Carbone, B. K. Kotowska and D. Kotowski, *Phys. Rev. Lett.*, 2005, **95**.
4. R. Lin, Y. Wang, Q. Lu, B. Tang, J. Li, H. Gao, Y. Gao, H. Li, C. Ding, J. Wen, P. Wu, C. Liu, S. Zhao, K. Xiao, Z. Liu, C. Ma, Y. Deng, L. Li, F. Fan and H. Tan, *Nature*, 2023, **620**, 994-1000.
5. E. Ochoa-Martinez, M. Ochoa, R. D. Ortuso, P. Ferdowsi, R. Carron, A. N. Tiwari, U. Steiner and M. Saliba, *ACS Energy Lett.*, 2021, **6**, 2626-2634.
6. H. B. Lee, N. Kumar, B. Tyagi, K.-J. Ko and J.-W. Kang, *Sol. RRL*, 2020, **5**.
7. Y. Yao, J. Zhang, H. Su, Y. Li, N. Li, T. Nie, L. Liu, X. Ren, N. Yuan, J. Ding and S. Liu, *Sol. RRL*, 2022, **7**, 2201025.
8. Y. Wang, J. Song, J. Ye, Y. Jin, X. Yin, Z. Su, L. Hu, Y. Wu, C. Qiu, H. Wang, W. Yan and Z. Li, *Chem. Commun.*, 2023, **59**, 6580-6583.
9. S. Gharibzadeh, P. Fassl, I. M. Hossain, P. Rohrbeck, M. Frericks, M. Schmidt, T. Duong, M. R. Khan, T. Abzieher, B. A. Nejand, F. Schackmar, O. Almora, T. Feeney, R. Singh, D. Fuchs, U. Lemmer, J. P. Hofmann, S. A. L. Weber and U. W. Paetzold, *Energy Environ. Sci.*, 2021, **14**, 5875-5893.
10. W. Chen, Y. Wang, G. Pang, C. W. Koh, A. B. Djurišić, Y. Wu, B. Tu, F. z. Liu, R. Chen, H. Y. Woo, X. Guo and Z. He, *Adv. Funct. Mater.*, 2019, **29**.
11. L. Zhang, Q. Kang, Y. Song, D. Chi, S. Huang and G. He, *Sol. RRL*, 2021, **5**.
12. W. Wang, Q. Zhou, D. He, B. Liu, L. Bai, C. Xu, Q. Song, P. Zhao, C. Chen, K. Sun, H. Yang, Z. Zang, D. Lee and J. Chen, *Sol. RRL*, 2021, **6**, 2100893.
13. H. Luo, F. Tu, X. Chen, L. Xing, L. Cao, G. Ren, S. Ji, Y. Zhong, L. Xiao, W.-C. Chen, Q.-D. Yang, C. Yang and Y. Huo, *J. Mater. Chem. A*, 2023, **11**, 8791-8797.
14. C. Song, X. Li, Y. Wang, S. Fu, L. Wan, S. Liu, W. Zhang, W. Song and J. Fang, *J. Mater. Chem. A*, 2019, **7**, 19881-19888.
15. Y. B. Gao, Y. J. Wu, Y. Liu, M. Lu, L. L. Yang, Y. H. Wang, W. W. Yu, X. Bai, Y. Zhang and Q. L. Dai, *Nanoscale Horiz*, 2020, **5**, 1574-1585.